

Bio-Mediated Synthesis of ZnO Nano Photocatalyst using *C. gigantea* (L.): Microstructural Study for Rapid Degradation of Organic Pollutants from Aqueous Medium

Goutam Mandal, Baibaswata Bhattacharjee

Received 11 June 2024, Accepted 25 August 2024, Published on 18 October 2024

ABSTRACT

The purpose of this paper was to synthesize ZnO nanoparticles (NPs) from *Calotropis gigantea* (L.) and use them as photocatalyst for the elimination of wastewater contaminants, methyl orange (MO), and paracetamol (PCM) by UV irradiation. The UV-Vis absorption spectra show a peak at a wavelength of 374 nm with excitonic band gap of 3.41 eV. The hexagonal unit cell with mean crystallite size of 29.13 nm was found from the XRD pattern. The FESEM images confirm the formation of nanostructures. The bio-mediated nanoparticles are used as nano photocatalysts to eliminate MO and PCM. The effects of irradiation time, photocatalyst dose, dye concentration, and solution pH on photodegradation were studied in MO. Furthermore, the photodegradation

of paracetamol was also investigated.

Keywords Bio-mediated synthesis, ZnO nanoparticle, Photocatalysis, Methyl orange (MO), Paracetamol (PCM).

INTRODUCTION

The shortage of drinking water resources caused by global warming stands a significant danger to humanity (Arthanareeswari *et al.* 2019). This impacts the ecology, adversely affecting agriculture and the local economy. Therefore, we face two critical obstacles to ensuring an adequate pure water supply and effectively recycling wastewater. The water supplies are extensively contaminated due to several factors. One of these factors is the discharge of chemical waste from dye factories, which exhibits more excellent chemical stability and long-lasting presence in the environment. Staining dyes are used in various sectors, such as textiles, paper and pulp, cosmetics, pharmaceuticals, food coloring, paints, leather tanning, and hair colorants (Zhu *et al.* 2011).

Azo dye, particularly methyl orange (MO), also known as dimethyl amino azo benzenesulfonate, is a water-soluble organic synthetic dye and has remarkable colorability and produces a vivid orange hue when dissolved in water (Behera and Behera 2022). Because of its extraordinary chemical endurance, MO is mostly utilized in the food, synthetic leather,

Goutam Mandal¹

Associate Professor

¹Present Affiliation: Department of Physics, BZSM Mahavidyalaya, Bankura 722101, West Bengal, India

¹PhD Research Scholar, Department of Physics, Bankura University, Bankura 722146, West Bengal, India

Baibaswata Bhattacharjee^{2*}

²Associate Professor, Department of Physics, Ramananda College, Bishnupur, Bankura 722122, West Bengal, India

Email: baib23@gmail.com

*Corresponding author

paper, and textile industries (Selvaraj *et al.* 2021). To mitigate the detrimental impact of these pollutants on the environment and comply with rigorous environmental standards, research on the removal of azo dyes in wastewater has been intensified.

On other hand, paracetamol is contemplated one of the most serious pollutants in wastewater (Izadi *et al.* 2020). The existence of pharmaceutical residues in wastewater has resulted in substantial degradation of the quality of both groundwater and surface water, therefore impacting both human well-being and the ecosystem (Abdel-Shafy and Mohamed-Mansour 2013). These biproducts are either directly or indirectly, damage the biological hierarchy.

Despite the development of different technologies such as adsorption, filtration, sedimentation, and biological treatment, these techniques are inadequate for complete water purification. Therefore, there is a substantial need for water filtration systems that are both secure and cost-effective. One of the most effective techniques is photocatalysis. Techniques that employ UV or visible light are categorized as advanced oxidation processes because of their very effective oxidizing capabilities (Baruah *et al.* 2010). In photocatalysis the semiconductor nanoparticles are used as photocatalyst (Pereira *et al.* 2014).

Many advantages may be achieved by using semiconductor nanoparticles (NPs) as a catalyst in wastewater treatment processes. Efficiency gains, cost reductions, and proper recycling are among these (Xiao *et al.* 2017). Among the several oxides of metals, zinc possesses the following desirable properties: A large surface area, great catalytic activity, a wide band gap, excellent chemical and structural stability, and negligible toxicity (Mensah *et al.* 2022).

Several physical and chemical approaches are utilized to fabricate ZnO NPs with different physical and morphological properties (Raha and Ahmaruzzaman 2022). However, due to hazardous ingredients, the need for extremely high temperatures and pressures, the expensive cost, and the long time required, research is increasingly focusing on clean and environmentally acceptable synthesis techniques (Gupta *et al.* 2023). Plants, plant extracts, and mi-

crobes are currently being used to produce metal and metal oxide nanoparticles in a simple, cost-effective, green method. However, plant-mediated synthesis with plants and plant extracts was preferred over other microbes owing to its convenience of use, large-scale facilitation, and safe production with no toxic byproducts (Patel 2022). Furthermore, plant components and extracts serve as natural reducing and capping agents. As a result, researchers have focused greatly on the bio-mediated synthesis of ZnO NPs, and many scientists are working on it. Various plants and their leaf extracts have been used to manufacture ZnO NPs (Akintelu and Folorunso 2020).

With these factors, the current study employed the bio-mediated approach to produce ZnO NPs using leaf extracts from *C. gigantea*. So far, our knowledge, the synthesized ZnO utilized as a nanoscale photocatalyst to remove contaminants from wastewater. The model pollutants used in this investigation were MO and PCM. The optimization of the photocatalysis of MO was done by changing operational parameters, including catalyst dose, starting dye concentration, and pH of the solution. Additionally, the process of photodegradation of paracetamol was examined by employing Zinc Oxide nanoparticles as a photocatalyst.

MATERIALS AND METHODS

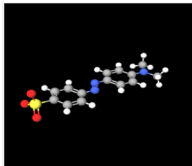
Materials

From Sigma-Aldrich Zinc acetate dihydrate and sodium hydroxide were purchased and used as received. The methyl orange dye was acquired from SRL, an Indian company. In the photodegradation experiment with MO dye, a concentration of 1.0 g/L stock solution was prepared and subsequently diluted with deionized water to change the concentration. Table 1 displays the chemical composition and characteristics of Methyl orange dye.

Collection of *C. gigantea*

C. gigantea leaves were obtained from the local region of Bankura (23.1645° N, 87.0624° E), West Bengal, India. The leaves were cleaned adequately in tap water before being washed with deionized water

Table 1. Properties of MO dye.

Material	Structure	λ_{\max} (nm)	MW (g/mol)	Molecular formula	Solubility (mg/L)
Methyl orange		464	327.33	$C_{14}H_{14}N_3NaO_3S$	200

and sliced with a clean table knife. The leaves were dried in a hot oven at 60°C for 8 hrs. Then they were ground into a powder and stored at room temperature in an airtight container until they were needed.

Preparation of leaf extract

6 g of the previously prepared dried leaf powder was mixed with 100 ml of deionized water and boiled the mixture at 60°C for 15 min. The solution was then cool down at room temperature before being passed through filter paper. After being collected in an amber container, the filtrate was stored in a deep freezer for future use.

Bio-mediated synthesis of ZnO nanoparticles

We utilized the bio-mediated synthesis method described in the paper of S. K. Chaudhuri and L. Malodia, with a few modifications (Chaudhuri and

Malodia 2017). Initially, stoichiometric amount zinc acetate dihydrate was dissolved in 35 ml of deionized water to make a solution with a concentration of 0.2 M, 15 ml of leaf extract of *C. gigantea* leaf extract was added to a zinc acetate solution under magnetic stirring. Afterward, 50 ml of 2M NaOH was added dropwise and stirring continued for the next 2 h. A white precipitate was formed at the end of the process which was filtered with filter paper. Washed the precipitate deionised water and ethanol by several times. This precipitate was dried up in 50°C about 3 h and calcinated at 300°C about 5 h. Finally, a fine powder was prepared using a ceramic pestle and mortar. The schematic synthesis process is explained in Fig. 1.

Characterization tools

A systronics AU2703 UV-Visible (double-beam) spectrophotometer was exploited to study the optical

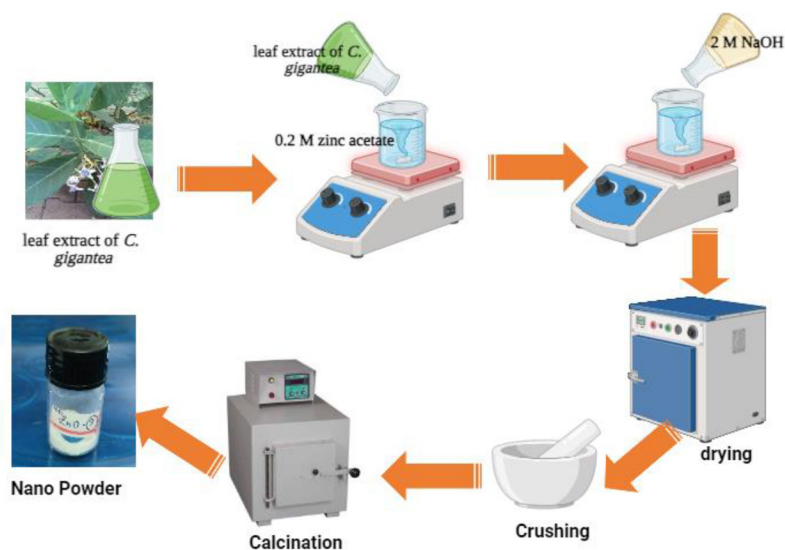


Fig. 1. Bio-mediated synthesis process of ZnO nano photocatalyst.

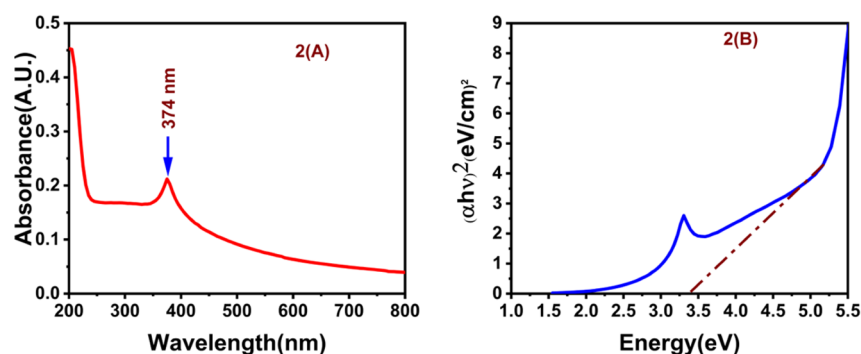


Fig. 2. (A) The UV-Vis spectra of ZnO nanostructures, (B) Band gap determination using Tauc's plot.

absorption spectra. In a Rigaku X-ray diffractometer, X-ray diffraction was tested using Cu-K α radiation at wavelength of 1.54 Å and with an angular range of 20°–80°. Using 5 kV accelerating voltages, a ZEISS made FESEM was used to analyze the surface morphology of the nanocrystal.

Photodegradation study

We conducted the photocatalytic experiment by evaluating the photodegradation rate of methyl orange

(MO) and paracetamol (PCM) in a 100 ml aqueous solution. To ensure adsorption-desorption equilibrium between contaminants and ZnO, the solutions were kept in the dark for 30 min. Under ultraviolet (UV) light, experiments were carried out. A spectrophotometer was used to record the UV-Vis absorption spectra of the reaction mixture at predetermined intervals to monitor the reaction's progress. The change in absorption at $\lambda_{max} = 464$ nm (MO) and $\lambda_{max} = 243$ nm (PCM) was then monitored. The rate of dye degradation was examined by varying operational factors

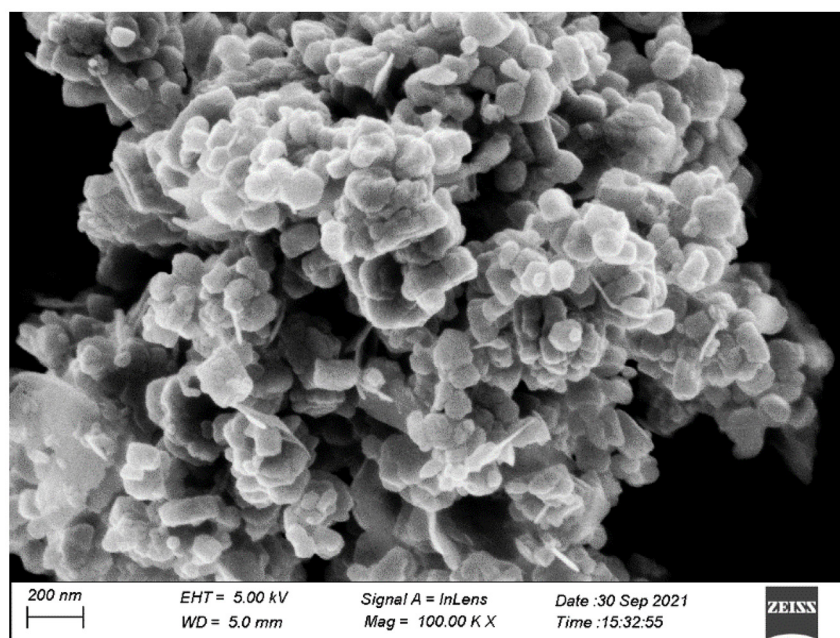


Fig. 3. FESEM image of ZnO nano photocatalyst.

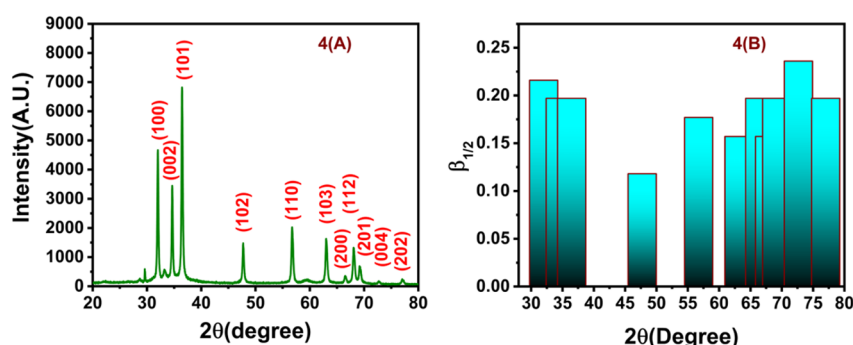


Fig. 4. (A) The XRD pattern of ZnO nanocrystal, (B) Half-width ($\beta_{1/2}$) vs. peak position (2θ) plot.

such as illumination interval, quantity of catalyst, concentration of dye, and pH of the solution. Variation of pH of the solution was done with the adding of 0.1M HCl or NaOH.

The degradation efficiency (D) or performance was computed using the given equation (Meng *et al.* 2009) :

$$D\% = (C_0 - C_t) / C_0 \times 100 \quad (1)$$

Here, C_0 and C_t are the initial concentration and concentration of the pollutant after t min of irradiation.

RESULTS AND DISCUSSION

Optical properties

The UV absorption spectra shows that the highest

absorption peak of ZnO at 375 nm (Fig. 2(A)). The band gap (E_g) of the nanoparticles was estimated using Tauc equation (Tauc *et al.* 1966) and given by :

$$(\alpha h\nu)^2 = B (h\nu - E_g) \quad (2)$$

Here α : Absorption coefficient, h : Planck's constant, ν : frequency, and B : band tailing parameter. Here, band gap energy E_g was computed from the straight part on the abscissa of the graph of $(\alpha h\nu)^2$ vs. $h\nu$ is depicted in Fig. 2(B). The calculated band gap is 3.41 eV.

Structural analysis

FESEM

FESEM analysis was used to investigate the surface morphology, size, shape, and growth process of ZnO nanoparticles (Fig. 3). Nanoparticles seem almost

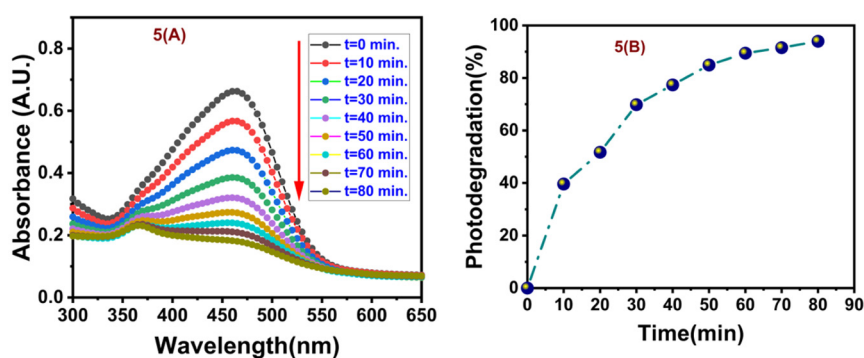


Fig. 5. The UV-Vis absorption spectra of (A) MO pollutant (concentration 15 mg/L) on irradiation with UV light for about 80 min, (B) Photodegradation percentage of MO with time.

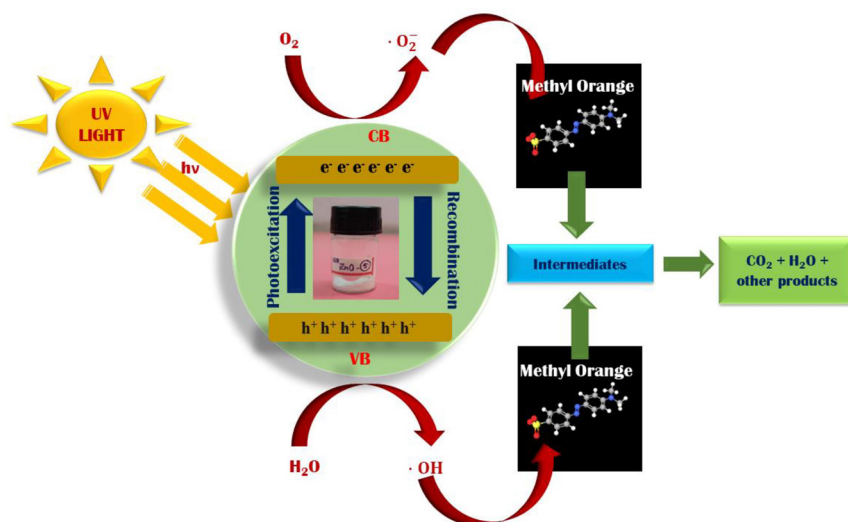


Fig. 6. The schematic diagram for photodegradation of MO dye.

spherical and orientated haphazardly in the FESEM picture.

XRD study

The XRD pattern of the ZnO nanocrystal (see Fig. 4 (A)) reveals that the unit cell was hexagonal structure. The graph exhibits maxima that correspond to the (100), (002), (101), (102), (110), (103), (200), (112), (201), (004), and (202) crystallographic planes at different 2θ angles. Crystallographic planes are ar-

bitrarily oriented and well indexed to the hexagonal (wurtzite) structure with space group P63mc. The lattice constants are $a = b = 3.242 \text{ \AA}$ and $c = 5.188 \text{ \AA}$ and (Klingshirn 2007). Peaks are well matched with JCPDS file no. 96-210-7060. Fig. 4 (B) shows the FWHM or half-width ($\beta_{1/2}$) vs. 2θ . The FWHM of each diffraction peak was determined using Gaussian fitting.

The highest peak intensity at $2\theta = 36.468 \text{ \AA}$ with (101) Miller plane was used to determine the different crystallographic parameters. The Debye-Scherrer formula (Mandal and Bhattacharjee 2024) was employed to calculate size of the crystallite (D_V), dislocation density (δ_D), and microstrain (ϵ_m) of ZnO nanocrystal using the following equations :

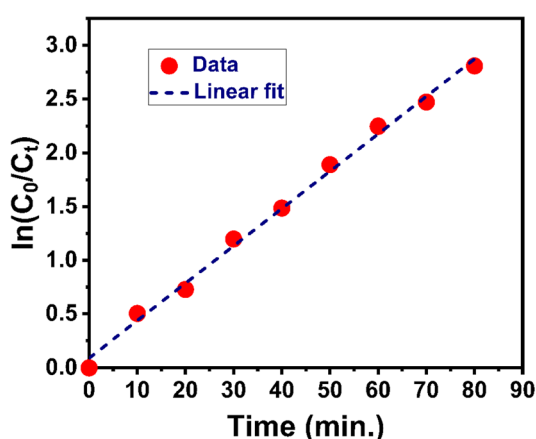


Fig. 7. Plot to determine the rate constant of MO dye (concentration 15 mg/L).

$$D_V = \frac{k\lambda}{\beta_{1/2} \cos\theta} \quad (3)$$

$$\delta_D = \frac{1}{D_V^2} \quad (4)$$

$$\epsilon_m = \frac{\beta_{1/2} \cos\theta}{4} \quad (5)$$

Here, K is 0.94 for the copper radiation.

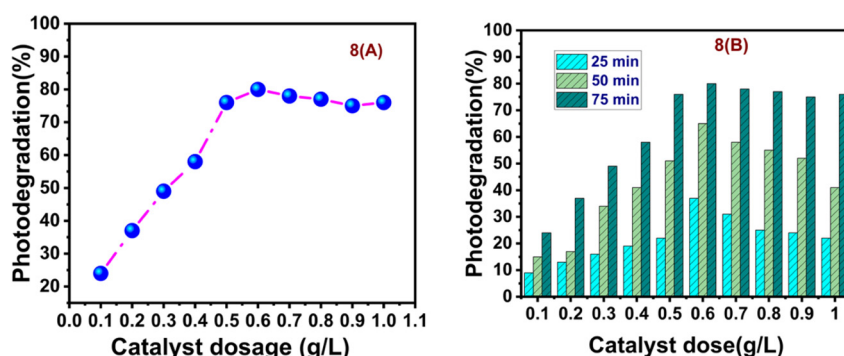


Fig. 8. (A) Effect of dosage on photodegradation (MO concentration 15 mg/L and pH:7), (B) Bar diagram of photodegradation vs. ZnO dosages at three different times.

The microstrain (ϵ_m) and crystallite size (D_v) was also calculated by the Williamson-Hall (W-H) equation (Mokoena *et al.* 2020) :

$$\beta_{1/2} \cos \theta = \frac{K\lambda}{D_v} + 4\epsilon_m \sin \theta \quad (6)$$

Table 2 provides the various crystal properties of the ZnO NPs synthesized using plant mediation.

Optimization of photocatalytic performance using MO dye

Effect of illumination time

Fig. 5 (A) displays the photodegradation of MO dye at a concentration of 15 mg/L with ZnO photocatalyst concentration of 0.5 g/L (pH at 7) under UV light. Degradation as a percentage of MO with irradiation duration ; following 80 minutes, it reached 93.26%. Fig. 5 (B) shows illumination time versus photodeg-

radation efficiency curve. During the initial stages of photodegradation, a higher concentration of excited electrons and oxidizing radicals was linked to the existence of many receptor sites (Saad *et al.* 2020). This enhanced the quick breakdown of MO molecules. As the irradiation period increased, considerable oxidizing radicals were consumed continuously, dropping the rate until equilibrium was attained significantly (Dong *et al.* 2011).

When the energy of the incident photon (E) exceeds band gap (E_g) of ZnO electron-hole pair (EHP) are generated. The mechanism of photodegradation of MO dye is given below :

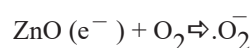


Table 2. Different crystal parameters.

Scherrer's method (considering (101) plane)			Williamson-Hall method		
Grain size (D_v)	Microstrain (ϵ_m)	Dislocation density (δ_d)	Grain size (D_v)	Microstrain (ϵ_m)	Dislocation density (δ_d)
29.13 nm	0.000816	$0.509 \times 10^{-3} / \text{nm}^2$	44.32 nm	0.000719	$0.532 \times 10^{-3} / \text{nm}^2$

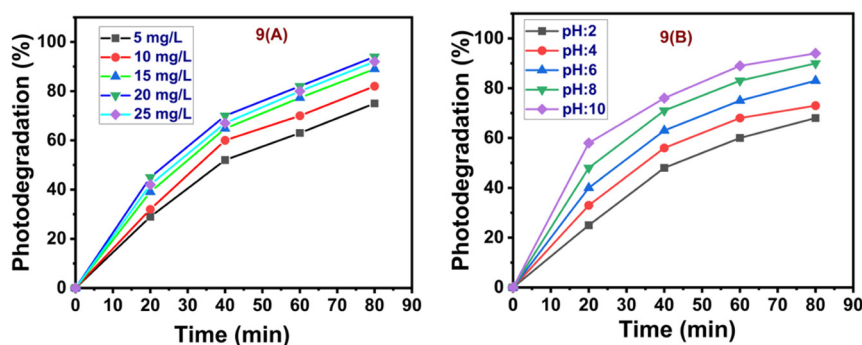
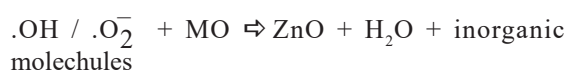
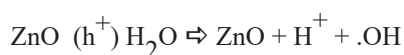


Fig. 9. (A) Effect of MO concentration on photodegradation (Photocatalyst dose 0.6 g/L with pH:7), (B) Effect of pH on photodegradation (Photocatalyst dose 0.6 g/L and Mg dose 20 mg/L) under irradiation time for 80 min.



The mechanism of photodegradation of MO dye is schematically shown in Fig. 6.

Degradation kinetics

The Langmuir-Hinshelwood model (Deflaoui *et al.* 2021) says that the rate of photodegradation follows pseudo-first order (PFO) dynamics. The rate constant (κ) of the photodegradation was determined using the following equation :

$$\ln \left(\frac{C_t}{C_0} \right) = \kappa t \quad 7$$

The kinetics of photodegradation is depicted in Fig. 7. The rate constant was calculated by linear least square fit. In our study, the rate constant of MO dye was 0.03477 min^{-1} .

Effect of photocatalyst dosage

The dose of photocatalysts has a crucial function in the dye degradation process. An experiment was done to investigate the impact of different dosage of photocatalysts on the photodegradation of MO dye.

The ZnO dosage was adjusted between 0.1 and 1.0 g/L (in steps of 0.1 g/L) keeping MO concentration at 15 mg/L and pH at 7 (see Fig. 8 (A)). The plot indicate that percentage degradation rises as the applied dosages increase from 0.1 g to 0.6 g. Significant deterioration was seen when the catalyst load exceeded 0.6 g/L. Fig. 8 (B) shows the bar diagram of photodegradation at three different time intervals (25 min, 50 min and 75 min) with nano photocatalyst dosage. According to the literature, the factors contributing to the observed results may include the increase in surface area, the availability of active catalytic sites, and the enhanced adsorption capabilities of the composites. This relationship was observed as the dosages employed increased (Qiu *et al.* 2022).

Effect of the initial dye concentration

The impact of varying the initial MO dye concentration on photodegradation was evaluated by adjusting the dye concentration from 5 mg/L to 25 mg/L while maintaining an optimum ZnO catalyst loading of 0.6 mg/L, a pH of 7, and an irradiation time 80 min. The results show that photodegradation initially increases with MO concentration and reaches an optimal value at 20 mg/L as shown in Fig. 9 (A). Increasing the dye concentration beyond the ideal value reduces photodegradation. This may be due to the hindering of light photon penetration in the solution, that blocks the photons from coming the surface of ZnO. Consequently, there was a reduction in the quantity of photogenerated EHP, which in turn led to a drop in photodegradation (Ambigadevi *et al.* 2021). In a

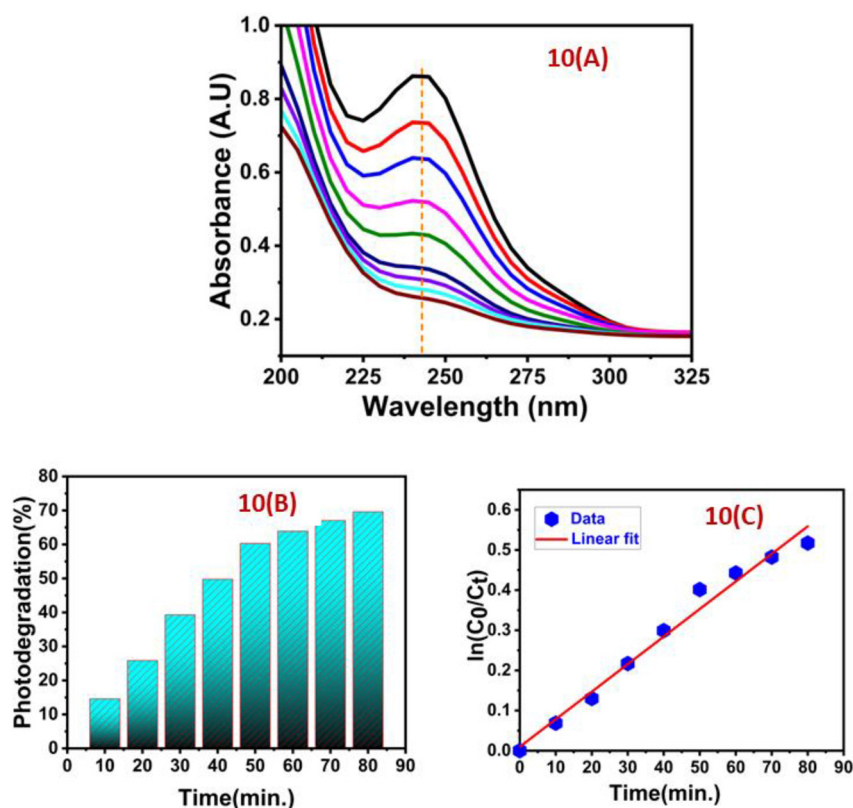


Fig. 10. (A) Photodegradation of paracetamol on irradiation with UV light about 60 min. (B) Photodegradation percentage of paracetamol with time (C) Plot to determine the rate constant.

similar manner, the enhanced concentration of dye molecules effectively obscured a significant portion of the catalyst's active sites on its surface.

Effect of pH of the solution

Another crucial operational parameter that influences the photocatalytic breakdown of wastewater pollutants is the pH of the solution. The photocatalytic activity of the catalyst can be affected by the nature of the pollutant, namely its acidity or alkalinity. Hence, it is essential to thoroughly investigate the impact of pH (Bagheri *et al.* 2017). A study was carried out to investigate the impact of pH within the pH range of 2-10, using the optimum amounts of photocatalyst (0.6 g/L) and MO dye (20 mg/L). The duration of irradiation was 80 min. The photodegradation was highest in the alkaline medium, as shown in Fig. 9

(B). In a highly alkaline solution, the dye is eliminated by adsorption. Therefore, a very alkaline solution promotes the preference for adsorption rather than photodegradation.

Photodegradation of PCM

Research was conducted to investigate the photodegradation of PCM. An aqueous solution containing paracetamol at 80 mg/L was created to do this. This solution was then combined with ZnO at a concentration of 0.5 g/L. Fig. 10 (A) illustrates the process of photodegradation. The deterioration of phase change material (PCM) was analyzed by collecting UV absorption data at 10 min intervals for 80 min. The percentage degradation of the PCM was then determined based on these measurements. Fig. 10 (A) demonstrates a direct correlation between the increase

in irradiation duration and the corresponding rise in the percentage deterioration. The PCM experienced a deterioration rate of 78.28% after being exposed to irradiation for 60 minutes. The Fig. 10 (B) provides information on the relationship between the duration of illumination and the effectiveness of ZnO removal. The rate constant for the photodegradation of PCM may be calculated using the graph in Fig. 10 (C). The rate constant obtained from the linear fitting was 0.00987 m^{-1} .

CONCLUSION

We have efficiently synthesized ZnO nanoparticles by utilizing the leaf extract of *C. gigantea*. Formation of spherical nanoparticles was verified using FESEM analysis. The optical band gap was determined based on the UV absorption data. The estimated value for the band gap was determined to be 3.41 eV. The XRD investigation showed presence of a hexagonal unit cell with a crystallite size of 29.13 nm. The synthesized ZnO from the leaf extract of *C. gigantea* was utilized for the first time to degrade two contaminants that are present in wastewater. Approximately 95% of the MO dye and 78% of the PCM were degraded after 80 min and 60 min when exposed to UV irradiation. Therefore, the newly synthesized bio-mediated ZnO nanoparticles have the potential to degrade harmful dyes rapidly and may be effectively employed in wastewater treatment.

ACKNOWLEDGMENT

The authors express their gratitude to the Physics Department, Bankura University and Bankura Zilla Saradhamani Mahila Mahavidyapith, Bankura.

REFERENCES

- Abdel-Shafy HI, Mohamed-Mansour MS (2013) Issue of pharmaceutical compounds in water and wastewater: Sources, impact and elimination. *Egyptian Journal of Chemistry* 56 (5) : 449—471.
<https://dx.doi.org/10.21608/ejchem.2013.1123>.
- Akintelu SA, Folorunso AS (2020) A review on green synthesis of zinc oxide nanoparticles using plant extracts and its biomedical applications. *BioNano Science* 10 (4) : 848—863.
<https://doi.org/10.1007/s12668-020-00774-6>.
- Ambigadevi J, Kumar PS, Vo DVN, Haran SH, Raghavan TS (2021) Recent developments in photocatalytic remediation of textile effluent using semiconductor based nanostructured catalyst : A review. *Journal of Environmental Chemical Engineering* 9 (1) : 104881—104890.
<https://doi.org/10.1016/j.jece.2020.104881>.
- Arthanareeswari M, Devikala S, Sridharan M (2019) Green synthesis of zinc oxide nanoparticles using *Typha latifolia*. L leaf extract for photocatalytic applications. *Materials Today : Proceedings* 14: 332—337.
<https://doi.org/10.1016/j.matpr.2019.04.155>.
- Bagheri S, TermehYousefi A, Do TO (2017) Photocatalytic pathway toward degradation of environmental pharmaceutical pollutants: Structure, kinetics and mechanism approach. *Catalysis Science & Technology* 7(20) : 4548—4569.
<https://doi.org/10.1039/C7CY00468K>.
- Baruah S, Mahmood MA, Myint MTZ, Bora T, Dutta J (2010) Enhanced visible light photocatalysis through fast crystallization of zinc oxide nanorods. *Beilstein Journal of Nanotechnology* 1(1): 14—20.
<https://doi.org/10.3762/bjnano.1.3>.
- Behera A, Behera A (2022) Advanced plastic materials. *Advanced Materials : An Introduction to Modern Materials Science*. Springer, Cham.
https://doi.org/10.1007/978-3-030-80359-9_14.
- Chaudhuri SK, Malodia L (2017) Biosynthesis of zinc oxide nanoparticles using leaf extract of *Calotropis gigantea*: Characterization and its evaluation on tree seedling growth in nursery stage. *Applied Nanoscience* 7 (8) : 501—512.
<https://doi.org/10.1007/s13204-017-0586-7>.
- Deflaoui O, Boudjemaa A, Sabrina B, Hayoun B, Bourouina M, Bourouina-Bacha S (2021) Kinetic modeling and experimental study of photocatalytic process using graphene oxide/TiO₂ composites. A case for wastewater treatment under sunlight. *Reaction Kinetics, Mechanisms and Catalysis* 133: 1141—1162.
<https://doi.org/10.1007/s11144-021-02022-8>.
- Dong Y, Dong W, Cao Y, Han Z, Ding Z (2011) Preparation and catalytic activity of Fe alginate gel beads for oxidative degradation of azo dyes under visible light irradiation. *Catalysis Today* 175 (1) : 346—355.
<https://doi.org/10.1016/j.cattod.2011.03.035>.
- Gupta D, Boora A, Thakur A, Gupta TK (2023) Green and sustainable synthesis of nanomaterials : Recent advancements and limitations. *Environmental Research* 231: 116316—116324.
<https://doi.org/10.1016/j.envres.2023.116316>.
- Izadi P, Izadi P, Salem R, Papry SA, Magdoui S, Pulicharla R, Brar SK (2020) Non-steroidal anti-inflammatory drugs in the environment: Where were we and how far we have come ? *Environmental Pollution* 267: 115370—115382.
<https://doi.org/10.1016/j.envpol.2020.115370>.
- Klingshirn C (2007) ZnO: From basics towards applications. *Physica Status Solidi (b)* 244 (9) : 3027—3073.
<https://doi.org/10.1002/pssb.200743072>.
- Mandal G, Bhattacharjee B (2024) Cerium Oxide Nanoparticle-Papain Enzyme Bioconjugate: Synthesis, Characterization and Optical Absorption Study for Biomedical Applications. *Indian Journal of Science and Technology* 17 (13) : 1331—1339.
<https://doi.org/10.17485/IJST/v17i13.270>.
- Meng F, Song X, Sun Z (2009) Photocatalytic activity of TiO₂

- TiO₂ thin films deposited by RF magnetron sputtering. *Vacuum* 83 (9) : 1147—1151.
<https://doi.org/10.1016/j.vacuum.2009.02.009>.
- Mensah K, Mahmoud H, Fujii M, Shokry H (2022) Novel nano-ferromagnetic activated graphene adsorbent extracted from waste for dye decolonization. *Journal of Water Process Engineering* 45: 102—512.
<https://doi.org/10.1016/j.jwpe.2021.102512>.
- Mokoena TP, Tshabalala ZP, Hillie KT, Swart HC, Motaung DE (2020) The blue luminescence of p-type NiO nanostructured material induced by defects: H₂S gas sensing characteristics at a relatively low operating temperature. *Applied Surface Science* 525:146002.
<https://doi.org/10.1016/j.apsusc.2020.146002>.
- Patel M (2022) Green synthesis of nanoparticles: A solution to environmental pollution. In *Handbook of Solid Waste Management: Sustainability through Circular Economy* Singapore: Springer Nature Singapore.
https://doi.org/10.1007/978-981-16-4230-2_97.
- Pereira RA, Pereira MFR, Alve MM, Pereira L (2014) Carbon based materials as novel redox mediators for dye wastewater biodegradation. *Applied Catalysis B: Environmental* 144 : 713—720.
<https://doi.org/10.1016/j.apcatb.2013.07.009>.
- Qiu B, Shao Q, Shi J, Yang C, Chu H (2022) Application of biochar for the adsorption of organic pollutants from wastewater: Modification strategies, mechanisms and challenges. *Separation and Purification Technology* 300 : 121—925.
<https://doi.org/10.1016/j.seppur.2022.121925>.
- Raha S, Ahmaruzzaman M (2022) ZnO nanostructured materials and their potential applications: Progress, challenges and perspectives. *Nanoscale Advances* 4 (8) : 1868—1925.
<https://doi.org/10.1039/D1NA00880C>.
- Saad AM, Abukhadra MR, Ahmed SAK, Elzanaty AM, Mady AH, Betiha MA, Rabie AM (2020) Photocatalytic degradation of malachite green dye using chitosan supported ZnO and Ce-ZnO nano-flowers under visible light. *Journal of Environmental Management* 258 : 110043.
<https://doi.org/10.1016/j.jenvman.2019.110043>.
- Selvaraj V, Karthika TS, Mansiya C, Alagar M (2021) An over review on recently developed techniques, mechanisms and intermediate involved in the advanced azo dye degradation for industrial applications. *Journal of Molecular Structure* 1224: 129—195.
<https://doi.org/10.1016/j.molstruc.2020.129195>.
- Tauc J, Grigorovici R, Vancu A (1966) Optical properties and electronic structure of amorphous germanium. *Physica Status Solidi (b)* 15 (2) : 627—637.
<https://doi.org/10.1002/pssb.19660150224>.
- Xiao J, Lv W, Xie Z, Song Y, Zheng Q (2017) L-cysteine-reduced graphene oxide/poly (vinyl alcohol) ultralight aerogel as a broad-spectrum adsorbent for anionic and cationic dyes. *Journal of Materials Science* 52 : 5807—5821.
<https://doi.org/10.1007/s10853-017-0818-y>.
- Zhu HY, Fu YQ, Jiang R, Jiang JH, Xiao L, Zeng GM, Wang Y (2011) Adsorption removal of congo red onto magnetic cellulose/Fe₃O₄/activated carbon composite: Equilibrium, kinetic and thermodynamic studies. *Chemical Engineering Journal* 173(2): 494—502.
<https://doi.org/10.1016/j.cej.2011.08.020>.